Orthorhombic velocity model building and imaging of Luda field with WAZ OBC data

Bin Zhou[2], Joe Zhou[1], Lubo Liu[1], Fong Cheen Loh[1], Junjie Liu[1], Yi Xie[1], Zhiliang Wang[2] and Xiaodong Pu[3]*
[1]CGG; [2]CNOOC Ltd-Tianjin; [3]COSL

Summary

Ocean Bottom Cable (OBC) acquisition has become the new trend in Bohai area with the benefit of operational flexibility, better illumination, better multiple elimination and better S/N for the targets at middle to deep depth. However, the presence of azimuthal anisotropy can cause severe imaging challenges in the Wide Azimuth OBC data, particularly fault imaging which is sensitive to velocity accuracy. Fault imaging can be smeared and fault shadows can be observed within complex strike-slip fault systems if the azimuthal dependency of wave propagation is not properly honored. In this paper, we will present an orthorhombic model building flow and demonstrate with the Luda OBC data that our approach can successfully reconcile the structural discrepancies between seismic images from different azimuths and provide a clear and sharp fault image with the WAZ stacking process.

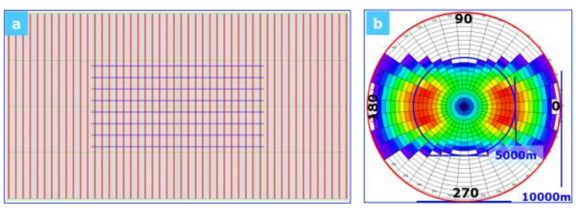

Figure 1: Wide azimugth orthogonal patch pattern used in Luda OBC acquistion (a) and offset-azimuth-fold plot for one patch (b): Radius of the diagram represents offset which is up to 10000m and each color-coded cell represents fold within a sector 10° x 500m.

Introduction

The Luda oilfield is located in the Liaozhong depression of Bohai with water depth ranging from 20m to 25m. The main reservoirs are sandstones in the Oligocene Dongying formation and Eocene Shahejie formation, which are compartmentalized by a complex strike-slip fault system. Data quality from the vintage towed streamer data suffers from serious noise and fault imaging issues especially at the reservoir level around 2s to 3.5s. This is one of the major challenges in hydrocarbon exploration and field development in this area. To better image the key aspect, a 3D-4C OBC survey was acquired in 2014 with a wide azimuth orthogonal patch pattern as shown in Figure 1. For each patch, eight 6000m-long cables were deployed on the water bottom with 400m cable separation; the source boat shot along the orthogonal direction with 250m shot line separation, resulting in a fold coverage of close to 200 and wide azimuth distribution as shown in Figure 1b.

The PSTM image from the OBC data shows obvious improvement in the S/N and continuity of the main reflectors however the fault image is smeared and the fault truncation is not clear. Strong azimuthal anisotropy can be observed in the common-offset common-azimuth gathers or the snail gathers by sorting traces in PSTM CIG gathers as a function of offset and then azimuth (Figure 2). The stacking response can be improved through azimuthal move-out correction (Hung et al, 2012), however it cannot mitigate the lateral discrepancies in the fault imaging. Orthorhombic depth imaging can remove azimuthal effects caused by subsurface structure thus allowing problems caused by azimuthal anisotropy to be addressed better and improving the fault imaging required for field development.

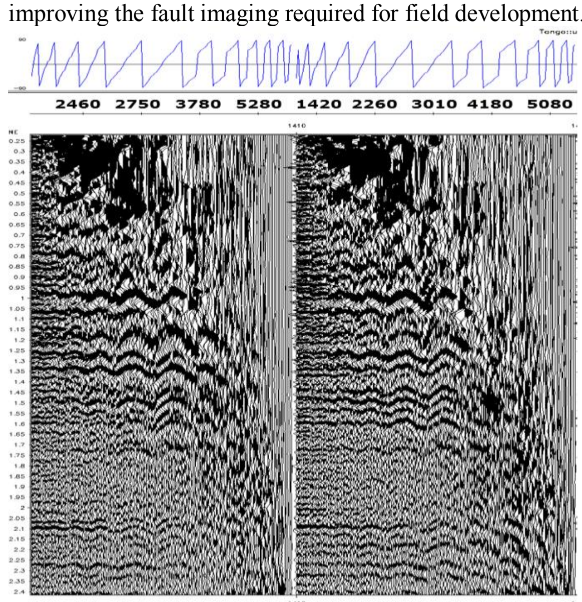

Figure 2: common-offset common-azimuth gathers (COCA) from the OBC PSTM with azimuth header overlaid above: obvious azimuthal residual moveout can be observed.

Orthorhombic velocity model building

In the WAZ model building approach, TTI velocity model building was performed with 3D CIG gathers in particular to make sure the azimuthal effect was not purely TTI-induced (Karazincir et al, 2014). However, a close look at the snail gathers shows that strong azimuthal effect can be observed from the shallow flat or gentle dipping events. An orthorhombic model has to be built for the shallow layers before we can build a meaningful TTI or Tilted

DOI http://dx.doi.org/10.1190/segam2015-5879535.1

orthorhombic (TORT) model for the complex structures in the deep.

Following Tsvankin (1997), Xie et al. (2012) it is proposed to compute the phase velocity for the orthorhombic media in the following form, which removes the weak anisotropy restriction:

$$\frac{V^2(\theta,\phi)}{V_{p_0}^2} = \frac{1}{2}\left(1 + 2\varepsilon(\phi)\sin^2\theta + \sqrt{(1+2\varepsilon(\phi)\sin^2\theta)^2 - 8(\varepsilon(\phi)-\delta(\phi))\sin^2\theta\cos^2\theta}\right)$$
$$\varepsilon(\phi) = \varepsilon_1\sin^4\phi + \varepsilon_2\cos^4\phi + (2\varepsilon_2+\delta_3)\sin^2\phi\cos^2\phi$$
$$\delta(\phi) = \delta_1\sin^2\phi + \delta_2\cos^2\phi \tag{1}$$

where $V(\theta,\phi)$ is the phase velocity with θ as ray polar angle; ϕ as the azimuth angle of ray relative to symmetry axis x_1 ; V_{P_0} , the vertical velocity of the P-wave; ε_2 , δ_2 , anisotropy parameters in the symmetry plane $x_1 - x_3$; ε_1 , δ_1 , anisotropy parameters in the symmetry plane $x_2 - x_3$; δ_3 , the anelliptic parameter of plane $x_1 - x_2$.

Based on equation 1 and with the a priori assumption that the direction (ϕ) of slow velocity axis (x1) is known, a single orthorhombic model can be built that reconciles the kinematics of the TTI models built from three angles. In the first stage of model building, three azimuth sectors (-10°, 45° and 135°) are selected. These azimuths are chosen to take advantage of the vintage velocity model (-10°) and the regional stress direction (~45°). For each azimuth sector, we select traces with azimuths within 15 degree of nominal azimuth angle for binning and regularization. After that, standard TTI model-building flow is applied for each azimuth sector to minimize the residual curvature in the gathers. Well velocities are used for calibration to make sure the vertical velocities from different azimuths are tied to the well velocities. Figure 3 shows the CIG gathers from all three azimuths with the same initial isotropic model and after three iterations of TTI velocity update, a clear convergence of gather curvature can be observed here.

Once satisfactory residual curvature from all three azimuths was reached for the shallow layers, we used Equation 1 to generate the initial orthorhombic model from the three TTI velocity fields. The initial slow velocity direction was set as 135 degrees and it was then refined by data fitting using elliptical assumption. From the result we can see that the azimuthal anisotropy mostly exist in the Pliocene and Miocene layers as shown in Figure 4a (up to 13% velocity difference), corresponding to the regional tectonic extrusion period between the end of Miocene and Pliocene. In the deep section, the δ_3 values found were negligible and didn't conform with geology, so these were clipped below Miocene layers. Figure 4b shows a depth slice in the Miocene formation of the extracted δ_3 volume which is clearly confined by the major fault planes.

In the second stage of model building, Orthorhombic ray tracing and tomographic update (Han and Xu, 2012) were applied to update the V_{P_0} . Residual curvature 3D CIG picking from the orthorhombic PSDM migrated gathers produced a good illumination, resulting in a high resolution velocity model (Figure 5), as opposed to picking on the single TTI PSDM result. Compared with the initial isotropic model, the final orthorhombic model provides much flatter and more symmetric 3D CIG gathers (Figure 6); the stack image also shows much sharper fault image since the structural discrepancies across different azimuths have been greatly reduced especially at the faulting area.

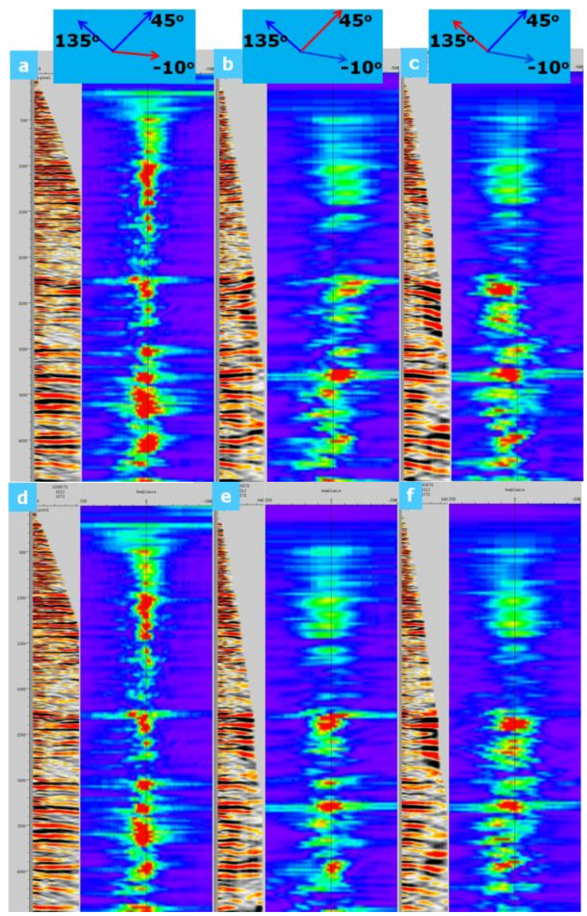

Figure 3: PSDM CIG gathers from all three azimuths with the same initial isotropic model (a,b,c) and after three iteration of TTI velocity update (d, e, f): a clear convergence of gather curvature can be observed.

DOI http://dx.doi.org/10.1190/segam2015-5879535.1

WAZ optimal stacking

To realize the full value of the WAZ acquisition and orthorhombic model building, the final migrated data need to be combined in a way that will overcome the issues from the varied illumination and S/N between different azimuths. Hung et al. (2012) proposed an optimal stacking method base on the concept of cross-correlation: the 3D CIG gathers are first flattened, and then the stacking weights for different azimuths are calculated by a cross-correlation process between a pilot and each input trace before stacking. This process can be iterated to get the optimal result. Compared with the conventional average stacking, this approach clearly provides better S/N and event continuity. The final WAZ OBC result was compared with the legacy towed streamer image (Figure 8), a step change in the imaging quality can be observed: sharp fault imaging, clear basement definition, high resolution and high Signal-to-Noise ratio in the target level.

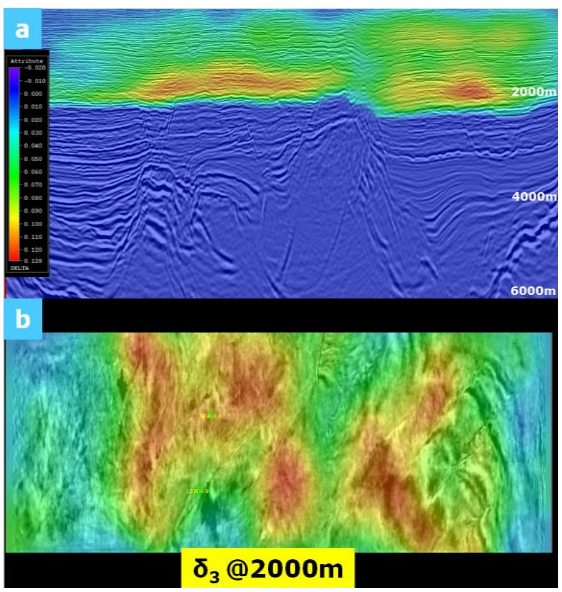

Figure 4: Vertical and depth slice of δ_3 volume: it was clearly confined by the major fault planes.

Impact on the interpretation and field development

In Figure 7, we compare a legacy PSTM section and the new WAZ OBC PSDM section passing through two wells (already converted to time domain). These wells were drilled based on old interpretation that the target reservoirs are connected at these two well locations. However, one well is a discovery and the other is totally dry. From the WAZ OBC result (Figure 8), the two wells are separated by a fault at the sand layers and are not connected.

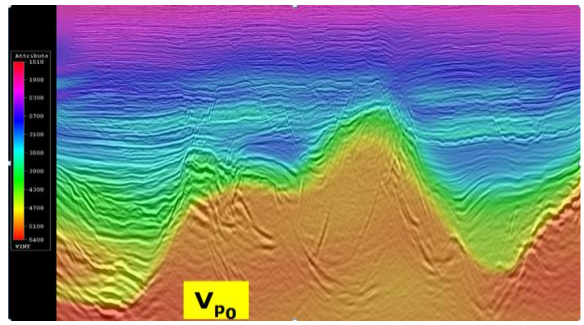

Figure 5: Vertical velocity after orthorhombic model update

Conclusions

To better image the Luda field's complex and steeply dipping fractures and the strike slip-fault systems, the first requirement is full azimuth seismic data. An accurate velocity model is another essential element. Any lateral-positioning error varying with offset and/or azimuth can make the final image suboptimal. We have demonstrated orthorhombic modeling/imaging can properly account for the influence of azimuthal anisotropy and provide important information for locating wells.

Compared with the isotropic model-based results, the orthorhombic model produced a much better depth image with clear boundary faults, and the flatness of gathers are improved across all azimuth directions. A Wide Azimuth (WAZ) optimal-stacking algorithm was used to produce the final image. The results show improved event continuity and imaging quality both in the fault system and also in the problematic, low S/N zone in the Bohai area.

Acknowledgments

The authors would like to thank CNOOC Ltd - Tianjin and CGG for the permission to present the data and publish this work.

DOI http://dx.doi.org/10.1190/segam2015-5879535.1

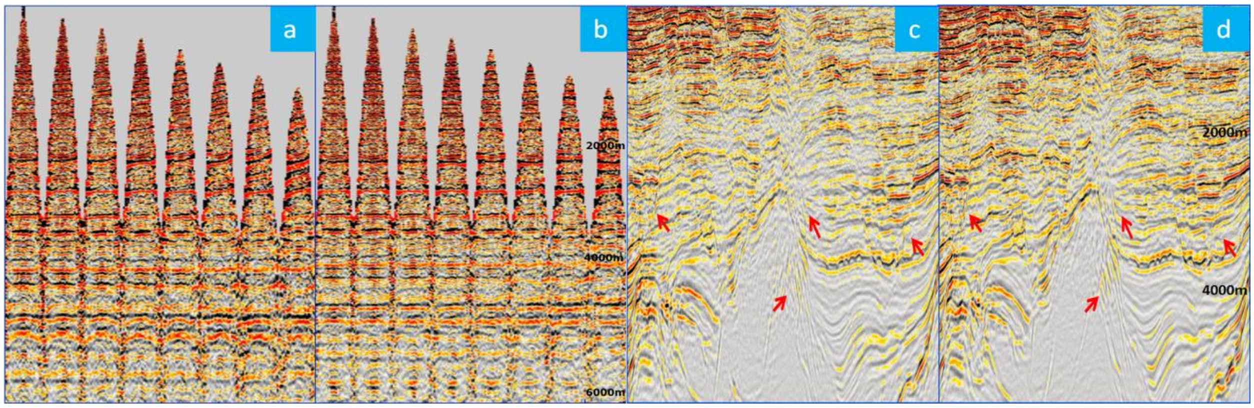

Figure 6: 3D PSDM CIG gathers (CDP-OFFSETY-OFFSETX) and stack comparison with (a) and (c) isotropic model and (b) and (d) final orthorhombic model: Wobbling effects from COCA TTI PSDM CIGs would be relevant for supporting orthorhombic workflow.

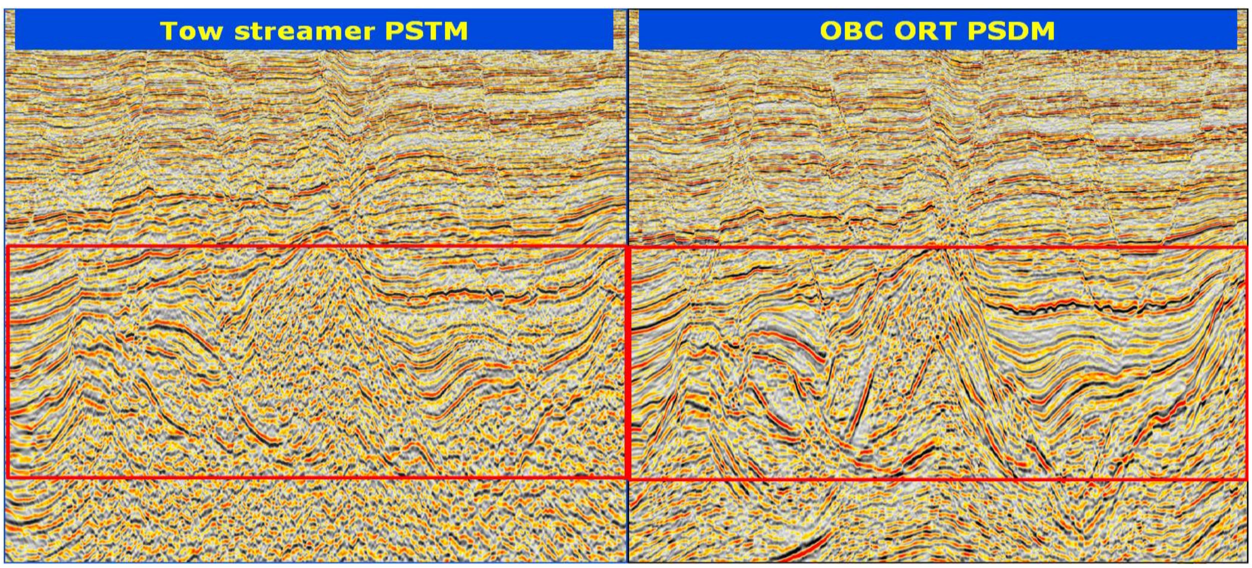

Figure 7: Legacy tow streamer PSTM stack vs. OBC ORT PSDM: better event continuity and fault definition.

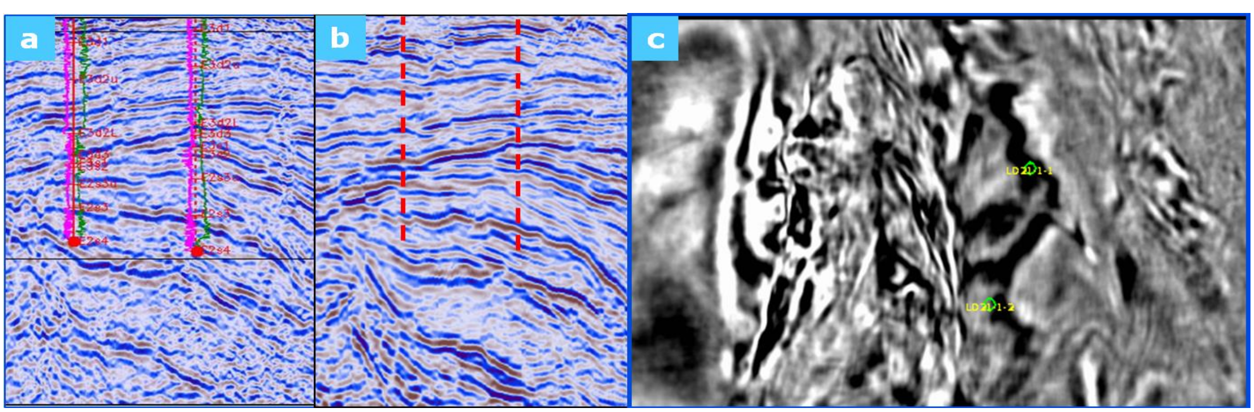

Figure 8: Seismic section passing through two wells and time slice, (a) legacy towed streamer PSTM, (b) and (c) OBC ORT PSDM, c): The WAZ OBC dats shows sharp fault imaging, clear basement definition and high resolution and S/N ratio at the target level.

DOI http://dx.doi.org/10.1190/segam2015-5879535.1

EDITED REFERENCES

Note: This reference list is a copyedited version of the reference list submitted by the author. Reference lists for the 2015 SEG Technical Program Expanded Abstracts have been copyedited so that references provided with the online metadata for each paper will achieve a high degree of linking to cited sources that appear on the Web.

REFERENCES

Han, W., Xu, S., Orthorhombic ray-tracing and traveltime calculation: Presented at the 74th Annual International Conference and Exhibition, EAGE.

Hung, B., Yin, Y., 2012, Optimal stacking for multi-azimuth prestack seismic data: ASEG Conference.

Karazincir, M., and R. Orumwense, 2014, Tilted orthorhombic velocity model building and imaging of Zamzama gas field with full-azimuth land data: The Leading Edge, **33**, 1024–1028. http://dx.doi.org/10.1190/tle33091024.1.

Tsvankin, I., 1997, Anisotropic parameters and P-wave velocity for orthorhombic media: Geophysics, **62**, 1292–1309. http://dx.doi.org/10.1190/1.1444231.

Xie, Y., Birdus S., Sun J., Notfors C., 2012, Prestack depth imaging of multi-azimuth seismic data in the presence of orthorhombic anisotropy: ASEG Conference.

DOI http://dx.doi.org/10.1190/segam2015-5879535.1